

See discussions, stats, and author profiles for this publication at: <https://www.researchgate.net/publication/269310033>


Hyperspectral image classification based on spectral-spatial features using probabilistic SVM and locally weighted Markov Random Fields

Conference Paper · February 2014
DOI: 10.1109/IranianCIS.2014.6802573

CITATIONS
12


READS
72

2 authors:



Mostafa Borhani
Sharif University of Technology
21 PUBLICATIONS **49** CITATIONS

SEE PROFILE




Hassan Ghassemian
Tarbiat Modares University
302 PUBLICATIONS **1,906** CITATIONS

SEE PROFILE

Some of the authors of this publication are also working on these related projects:



Data Fusion [View project](#)



Panchromatic and Multi-Spectral Image Fusion [View project](#)

Hyperspectral Image Classification Based on Spectral-Spatial Features Using Probabilistic SVM and Locally Weighted Markov Random Fields

Mostafa Borhani
Faculty of Electrical & Computer Engineering
Tarbiat Modares University
Tehran, Iran
m.borhani@modares.ac.ir

Hassn Ghassemian
Faculty of Electrical & Computer Engineering
Tarbiat Modares University
Tehran, Iran
ghassemi@modares.ac.ir

Abstract— The proposed approach of this paper is based on integration of the local weighted Markov Random Fields (MRF) on support vector machine (SVM) framework for hyperspectral spectral-spatial classification. Our proposed method consists of performing probabilistic SVM classification followed by a spatial regulation based on the MRF. One important innovation of this paper is the use of marginal weighting function in the MRF energy function, which preserves the edge of regions. The proposed spectral-spatial classification was examined with four real hyperspectral images such as aerial images of urban, agriculture and volcanic with different spatial resolution (1.3m and 20m), different spectral channels (from 102 to 200 bands) and different sensors (AVIRIS and ROSIS). The novel approach was compared with some pervious spectral-spatial methods such as ECHO and EMP. Experimental results are presented and compared with class map visualization, and some measurements such as average accuracy, overall accuracy and Kappa factor. The proposed method improves accuracy of classification especially in cases where spatial additional information is significant (such as forest structure).

Keywords— *Hyperspectral Spectral-Spatial Classification, Markov random fields, probabilistic SVM, local weighted marginal, remote sensing*

I. INTRODUCTION

Pixelwise classifiers for Hyperspectral image classification are solely applied on spectral features regardless of how classify the neighboring pixels. But in a real image, adjacent pixels are connected and interdependent [1], there are two reason for independency of neighbor pixels; first because the imaging sensors are receiving considerable energy from adjacent pixels and second reason is related to the similar structures in the scene image, those are usually greater than a pixel in size. This local information should help to properly interpret the landscape. So, for improving the classification accuracy, some novel spectral-spatial methods must be developed to allocate the correct class to each pixel by followed conditions:

1. Spectral characteristic of pixel (Spectral features)
2. The extracted information from its neighbors (Spatial features).

Landgrebe and his research group were the pioneered of introduction of spatial context in multi-band image classification. They introduced the well-known ECHO (Extraction and Classification of Homogeneous. Objects) [2]. We used ECHO in this paper as a standard technique for spectral-spatial classification. The ECHO classification originally are designed to identify objects in multispectral data, gather the statistics of the identified objects, and where possible, to classify the data on an object-by-object basis. ECHO includes spatial as well as spectral information in the classification algorithm and thereby increases the classification accuracy.

In this paper, a novel spectral-spatial classification method was proposed using the constant nearest neighbor to explore and analyze the dependencies between the pixels.

Probabilistic SVM and MRF respectively, are two powerful tools to classify the hyperspectral data and context analysis.

Bovolo [3] and Liu [4] had developed methods based on SVM and MRF, respectively, for the SAR and multi-spectral image classification (four bands). Authors used the MAP decision rule before the final decision, both of the papers employed SVM in order to estimate the class conditional PDF and MRF to estimate the location-based class. We extend this approach to the Hyperspectral data. Then, we proposed a new method based on MRF and SVM for Hyperspectral image classification. In the first step of the proposed method, the probabilistic SVM classification is applied [5] [6]. The second phase is the use of spatial data in order to refine the classification results obtained in the first phase. This is achieved by MRF Markov Random Fields. The significant differences with the previously proposed methods [7] [3] [4] are in the definition and integration of weighting function in MRF energy function to protect margins in the location, while procedures. The operational scheme of proposed classification method is shown in Figure 1. There is a B-band Hyperspectral image as input and which can be seen as a set of pixel vectors of n elements $X = \{X_j \in \mathbb{R}^B, j = 1, 2, \dots, n\}$. We remind that the classification involves assigning each pixel to one of the K classes $\{w_1, w_2, \dots, w_K\}$.

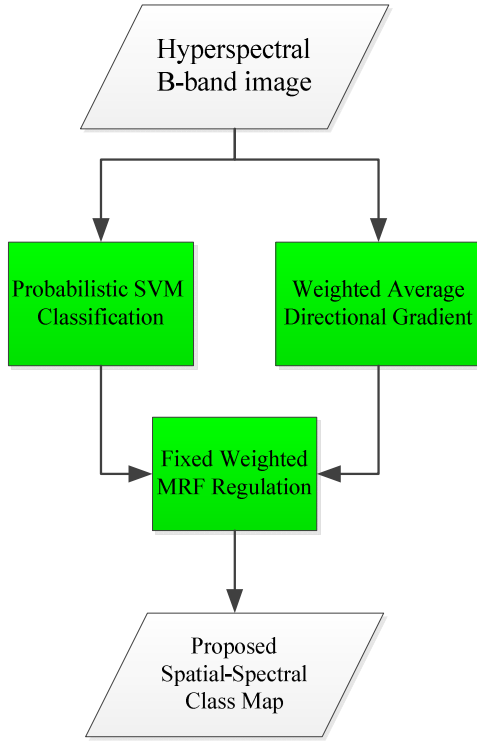


Figure 1. The proposed scheme based on probabilistic SVM and MRF

II. . PROBABILISTIC SVM CLASSIFICATION

The first step of the proposed process includes performing pixelwise probabilistic SVM in Hyperspectral Images [8] [9]. Other classifiers can also be used [10]. However, SVM is well suited for classification of Hyperspectral Data [10] [9]. The results are as follows:

1. Classification map; where each pixel has its own class label.
2. Estimation of the probability of each pixel belonging to each of the classes.

The standard SVM does not provide estimates of the probability of different classes. Two techniques for calculating estimates of the probability of multi-class classification is described in [6] and [5]. We recommend using one of the methods that have been implemented in the LIBSVM library [6]. Our goal is to estimate the probability of each pixel belonging to the target class:

$$p = \{p_k = p(y = k|X), k = 1, \dots, k\} \quad (1)$$

Therefore, the 'one against one' multi-class SVM classification strategy with Gaussian RBF kernel is executed. Pairwise class probabilities $r_{ij} \approx p(y = i|y = i \text{ or } j, x)$ are implemented using improved operations, such as [11] and [8].

$$r_{ij} \approx \frac{1}{1 + e^{A\hat{f} + B}} \quad (2)$$

Where A and B are obtained by minimizing the negative logarithm of the likelihood function using training data and the value of \hat{f} is estimated. In addition, the probabilities of (1) are calculated with the solving of the followed optimization problem:

$$\min_p \sum_{i=1}^K \sum_{j:j \neq i} (r_{ji}p_i - r_{ij}p_j)^2 \text{ subject to } \sum_{i=1}^K p_i = 1, p_i \geq 0 \forall i \quad (3)$$

This problem has a unique solution that can be obtained by solving a simple linear system as described in [5].

III. THE WEIGHTED AVERAGE DIRECTIONAL GRADIENT

Hyperspectral images of a single band gradient, is calculated independent of the stage. Gradients are transitions between areas that define the boundaries between objects and they have high levels on local minimums. In addition, the average of directional gradient is used to define the weighting function. B-band image gradient calculation approaches have been analyzed in [12] and [13].

In our proposed method we have used the following approach: First, we calculated the slope of horizontal, vertical and diagonal (respectively corresponding to the directions of zero, 90, 45 and 135 degrees) using masks Sobel [14], which each slope is calculated as the sum of the slope of each spectral channel. The overall gradient banding $\nabla(X) = \{p_j \in R, j = 1, 2, \dots, n\}$ is considered as average of these four directional slopes.

IV. FIXED WEIGHTED MRF REGULATION

In the last step, regulation of SVM classification map is implemented using MAP-MRF framework. This framework is based on the assumption of independence among pixels of class, meaning that it is likely that the pixel belongs to the class ω_i , then the adjacent pixels are belong to the same class. In this paper, we implement the generalized Metropolis-Hasting [20] stochastic relaxation with annealing algorithm to calculate the MAP estimate from the pixelwise classification maps [15] [16]. This Method is based on Bayesian approach and intended to minimize the overall image energy by repeated minimization energy process in the spatial domain [21]. $L = \{L_j, j = 1, 2, \dots, n\}$ is the set of class labels for the X image. We propose that the local energy associated with a given pixel X_i considered as following:

$$U(x_i) = U_{\text{Spectral}}(x_i) + U_{\text{Spatial}}(x_i) \quad (4)$$

where $U_{\text{Spectral}}(x_i)$, and $U_{\text{Spatial}}(x_i)$ are the observed spectral and spatial energy function respectively, those are is calculated on N_i local vicinity. (N_i is set of neighboring pixels of X_i which has been considered the 8 in our implement (a square with side 3)). Spectral energy function is defined as:

$$U_{\text{Spectral}}(x_i) = -\ln(P(x_i|L_i)) \quad (5)$$

where $P(X_i|L_i)$ is estimated by using binary probability estimates from multi-class "one against one" SVM results [4] [5]. Two different equations is proposed for the spatial energy function. We will start with the standard spatial energy formula [3] that is calculated as:

$$U_{\text{Spatial}}(x_i) = \sum_{x_j \in N_i} \beta (1 - \delta(L_i, L_j)) \quad (6)$$

where $\delta(\dots)$ is the Kronecker delta and β parameter controls the importance of spatial energy against the spectral energy in

equation (4). Equation $U_{spatial}(X_i)$ is proportional to the number of pixels X_i those are dedicated to one of the other classes except L_i .

This spatial energy equation is good, especially for images with large spatial structures. However, if the object is small and is displayed as a single pixel in the image, the model prefers to assign this pixel to the class of objects around it. In order to reduce the earlier spatial energy function bugs and maintaining margins and small structures on the classification map we propose to use weighting function such as (7). calculating the correct margin map for Hyperspectral image is a challenging task. For example, it may be build with applying a threshold to gradient image $\{p_j \in R, j = 1, 2, \dots, n\}$. Therefore, an appropriate threshold should be chosen. Instead of calculating the margin map, we suggest the definition of following function:

$$\varepsilon(x_i) = 1 - \frac{\rho_i}{\alpha + \rho_i} \quad 0 < \varepsilon(x_i) \leq 1 \quad (7)$$

where, $\alpha > 0$ is a parameter which controls the approximation margin threshold. When $p_j = 0$ (no margin), then $\varepsilon(X_j) = 1$. Increasing p_j leads to smaller and closer to zero $\varepsilon(X_j)$. Thus as innovation of this article, the spatial energy term is offered as:

$$U_{spatial}(x_i) = \sum_{x_j \in N_i} \beta \varepsilon(x_i) (1 - \delta(L_i, L_j)) \quad (8)$$

Both of the approaches for calculating spatial energy function (equation (6) and (8)) are used in experimental implementation of this paper.

Here, we summarize the proposed algorithm for optimizing the energy function: In each iteration, an image location (ie pixel X_i) is randomly chosen. Local spatial energy $U(X_i)$ is calculated by Equation (4). Then, a new class labels L_i^{New} is chosen randomly for new pixel X_i and a new local energy $U^{New}(X_i)$ is calculated. If the energy fluctuation is defined as $\Delta U = U^{New}(X_i) - U(X_i) < 0$, the new class labels goes out $X_i: L_i = L_i^{New}$. Otherwise, allocate a new class with probability $p = \exp(-\Delta U/T)$ is accepted. Here T is the control parameter of general [15]. The proposed algorithm, generalized Metropolis- Hasting algorithm to the weighted margin.

V. EXPERIMENTAL EVALUATION

Figures 2-5 and Tables I, II and III give the results of an empirical evaluation and comparison of the proposed spectral-spatial classification in Hyperspectral remote sensed image with four different datasets (urban, agricultural and volcanic), different spatial resolution (1.3m and 20m) and the number of distinct spectral channels (from 102 to 200 bands) with different sensors (AVIRIS imaging spectrometer and ROSIS).

Indian Pines Hyperspectral image has been recorded by the AVIRIS sensor from the vegetated area in northwest Indiana. Spatial dimensions of this image is 145×145 pixels, and the spatial resolution of each pixel is 20m. Twenty water absorption bands [17] were removed and only 200 bands has been used in our experiments. The ten classes have been

investigated and the number of training samples for each class and accuracy per class for various methods is given in Table I. A False composite image and different methods' classification results are shown in Figure 2.

Hekla image has been obtained by AVIRIS sensor over the area around the central volcano in Iceland [18]. The AVIRIS sensor collects reflected waves with wavelength from $0.4\mu m$ to $2.4\mu m$ and uses four sensors with 224-channel spectrometers. During data collection, spectrometers #4 did not work properly. All of the data recorded with the out of service sensor and the first band of other spectrometers (those channels were empty), were excluded from the dataset. Thus, the remaining 157 data channels were used for our tests. Spatial dimension of investigated image is 560×600 pixels. Twelve classes of land cover were examined and the number of instances of each class label and the accuracy of the different methods are described in Table II. Tri-band image with artificial colors and also the classification results of different methods are shown in Figure 3. in Indiana and Hekla Images, 50 samples from reference data are considered as training samples randomly for each class and the remaining samples formed the test set.

University of Pavia dataset has been recorded by ROSIS optical sensor over the metropolitan area, University of Pavia in Italy. This image has 340×610 pixels, with a spatial resolution of 1.3m per pixel. The number of captured data channels is 115 (with spectral range from $0.43\mu m$ to $0.86\mu m$). 12 channels were the most impaired deleted and the remaining 103 bands were used for experiments of this paper. Artificial composite color image and also the classification results of different methods were shown in Figure 4.

Center of Pavia dataset was recorded from an urban area by the sensor ROSIS. The image used for the experiments has 300×900 pixels with 102 spectral channels (13 channels with the most noise were excluded). Nine class labels of reference ground truth map with the number of labeled samples in each class are given in Table III. Classification results are shown in Figure 5. Thirty samples were randomly selected as training samples for each class.

TABLE I. ACCURACY OF INDIANA PINES DATASET FOR EACH CLASS FOR DIFFERENT METHODS, YELLOW BOXES IN ALL TABLES MEANS THE BEST ACCURACY AMOUNT ALL OF THE APPROACHES

Class	#	3-NN	ML	SVM	ECHO	Proposed Approach without/with Weighting	
1	1434	41.84	71.39	78.18	83.45	93.28	98.48
2	834	62.24	63.01	69.64	75.13	83.93	90.82
3	234	73.37	85.87	91.85	92.39	99.46	98.37
4	968	67.43	79.43	82.03	90.1	98.58	98.91
5	2468	53.91	52.65	58.95	64.14	82.09	76.92
6	614	64.72	85.99	87.94	89.89	97.7	97.34
7	54	84.62	48.72	74.36	48.72	97.44	97.44
8	497	86.35	93.51	92.17	94.18	97.54	97.54
9	747	91.97	94.69	91.68	96.27	97.7	97.56
10	26	100	36.36	100	36.36	100	100

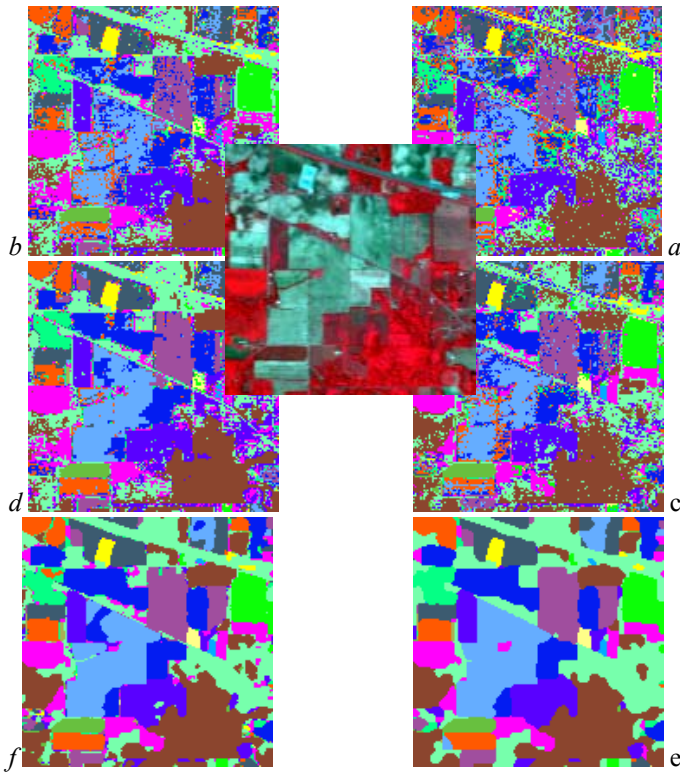


Figure 2. Indianan Pines, (middle) color combination of three bands 837, 636 and 537 nm, the results were classified as: (a) 3-NN, (b) ML, (c) SVM, (d) ECHO, (e) SVM with MRF, (f) SVM classifier with locally weighting MRF.

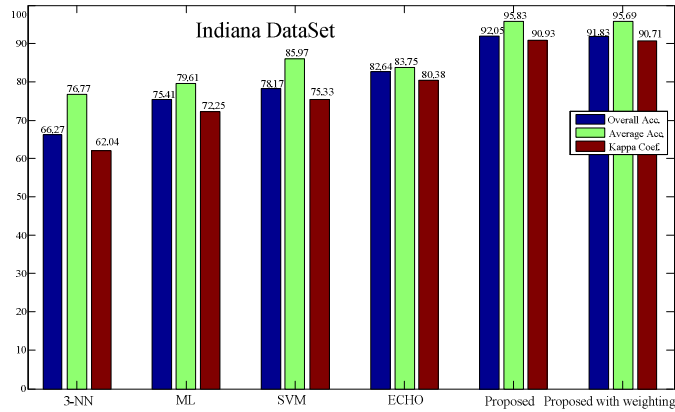


Figure 3. Indiana Pines dataset; The comparison of the accuracy, reliability and Kappa factor of the proposed method with previous methods.

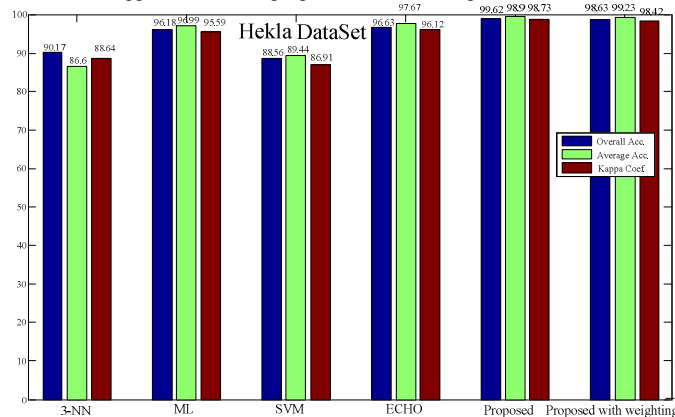


Figure 4. Hekla dataset; the comparison of the accuracy, validity, and Kappa factor of the proposed method with previous methods.

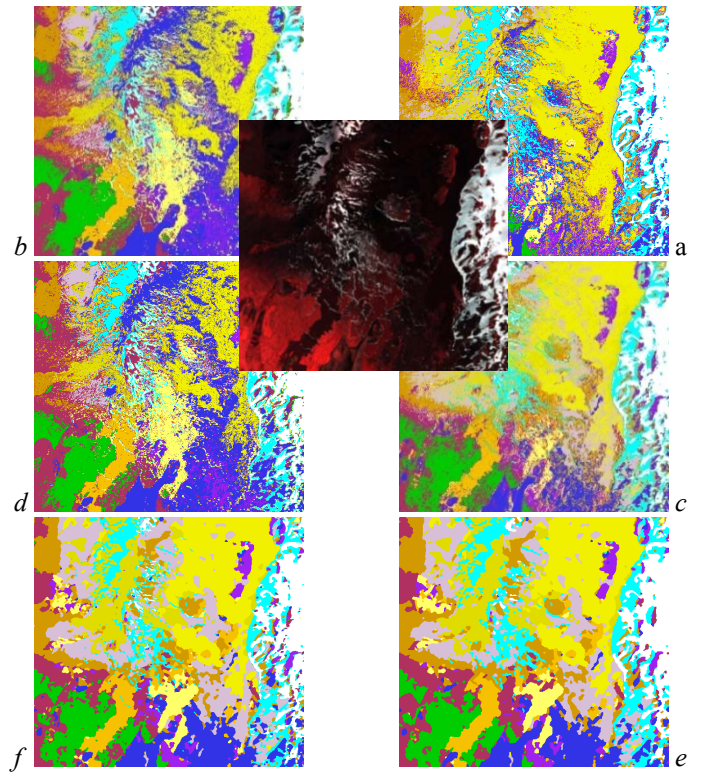


Figure 5. Hekla Image, (middle) Tri-band color combinations, 1125, 636 and 576 nm, (a) 3-NN, (b) ML, (c) SVM, (d) ECHO, (e) SVM classifier with MRF, (f) SVM classifier with locally weighting MRF.

TABLE II. ACCURACY OF HEKLA FOR EACH CLASS FOR DIFFERENT METHODS

Class	#	3-NN	ML	SVM	ECHO	Proposed Approach Without/with Weighting	
1	342	87.67	98.97	88.36	99.66	100	100
2	708	93.02	98.94	87.25	99.24	99.85	100
3	1496	92.39	94.26	88.24	94.26	100	100
4	2739	97.1	94.01	84.94	94.38	96.24	96.47
5	410	68.33	96.39	93.33	96.94	100	100
6	1023	91.98	98.15	94.24	98.25	100	98.97
7	684	87.07	98.74	87.54	99.37	100	100
8	700	82	96.15	91.69	96.31	99.38	99.38
9	404	86.44	92.37	85.88	95.48	100	100
10	550	55	97.6	74.2	99.6	100	97.8

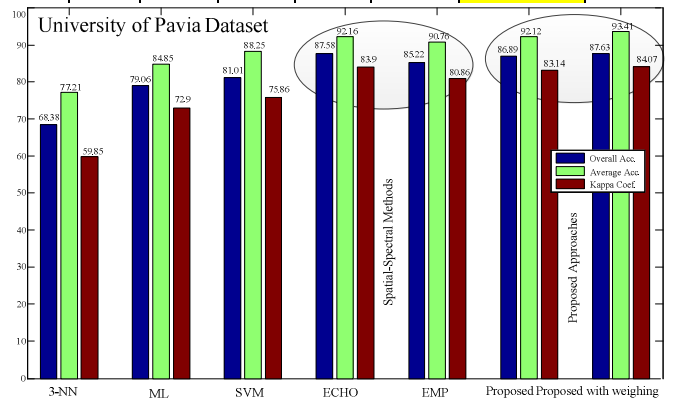


Figure 6. The comparison of the accuracy, validity, and Kappa factor of the proposed method with previous methods and EMP [19] and ECHO

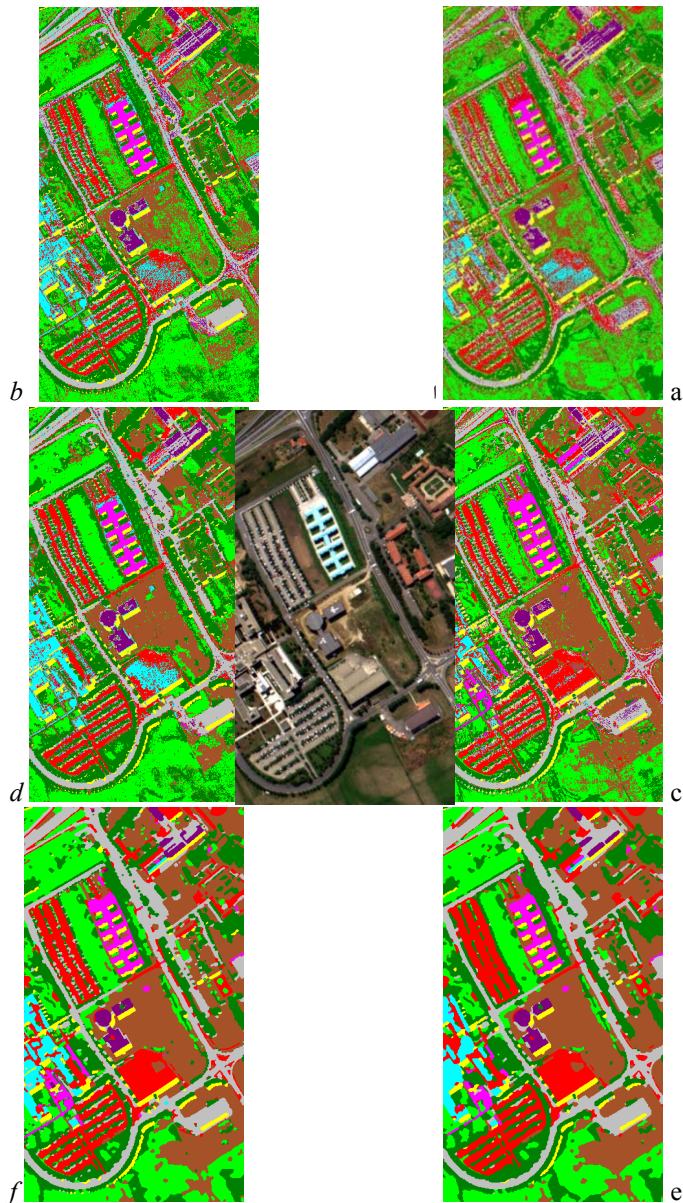


Figure 7. University of Pavia dataset, (middle) false color combinations, 650, 558 and 478 nm, Classification map of (a) 3-NN, (b) ML, (c) SVM, (d) ECHO, (e) SVM with MRF, (f) SVM classifier with locally weighting MRF.

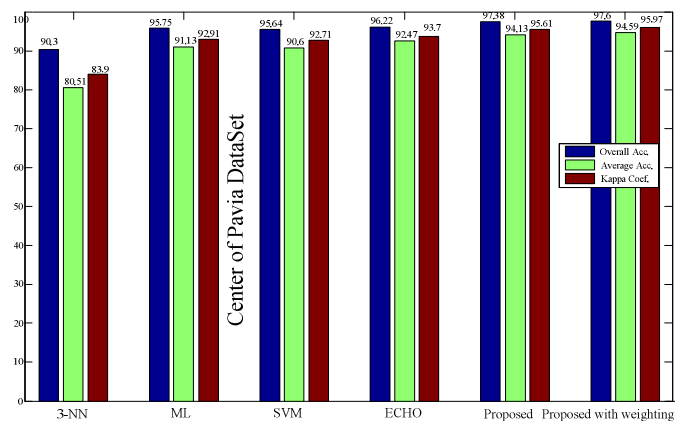


Figure 8. University of Pavia dataset; the comparison of the accuracy, validity, and Kappa factor of the proposed method with previous methods.

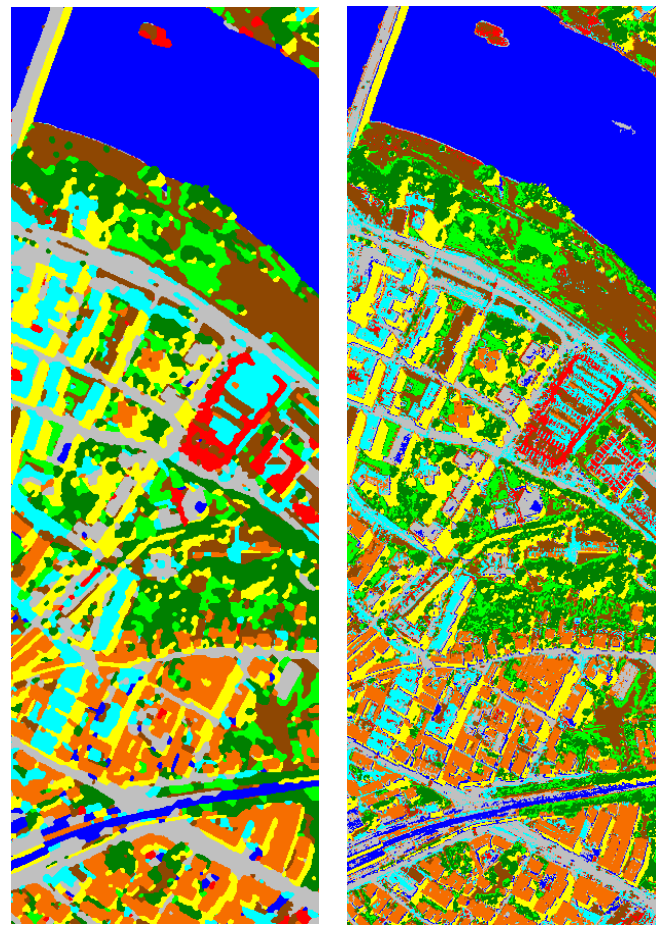


Figure 9. Center of Pavia dataset, (right) SVM, (left) proposed classifier with locally weighting MRF.

TABLE III. ACCURACY OF CENTER OF PAVIA PINES DATASET FOR EACH CLASS FOR DIFFERENT METHODS

Class	#	3-NN	ML	SVM	ECHO	Proposed Approach Without/with Weighting	
1	34352	98.87	99.35	99.78	99.35	100	100
2	2627	70.54	92.72	90.26	93.88	96.03	96.03
3	1788	90.16	87.14	96.42	88.17	99.66	100
4	2140	74.55	79.34	64.03	82.56	62.89	64.17
5	5365	79.16	90.03	88.38	91.13	94.64	95.11
6	5568	68.04	89.67	90.45	90.45	95.03	96.01
7	972	60.62	87.9	87.47	92.36	98.94	100
8	1112	93.16	95.66	98.71	95.93	100	100
9	2146	89.46	98.39	99.95	98.39	100	100

VI. DISCUSSIONS AND CONCLUSIONS

The proposed strategy of this paper is the use of SVM techniques within the closest vicinity based on the integration of the weighted MRF in the spectral classifications. Our proposed method consists of performing probabilistic SVM classification followed by a weighted MRF based spatial regulation. One of the important innovations is the integration method of weighting function in the energy function in Markov random fields, which seeks to maintain margins during spatial

uniformity. The proposed strategy with and without weighting method was examined on four real datasets and was compared with pixelwise methods such as 3-NN, ML and SVM classification methods and some spectral – spatial classification approaches such as ECHO and EPM [22].

As implementations show the proposed method creates good classification results for different types of images. However, as expected, the fixed nearest neighbor method did not extract small objects in the image correctly. Furthermore, due to the use of nearest neighbors, which contain a small number of pixels, the proposed method is useful only if a large area with wrong label pixels is not present in the original plans. If there is such an area, MRF-based methods cannot reconstruct the correct class label.

Experimental evaluations of the proposed method for spectral-spatial classification were provided in Figures 2-5 and Table I, II and III for the four hyperspectral images. Test results can be summarized as follows:

- SVM classification approach is suitable pixelwise method for large dataset with limited training samples.
- Examination of the spatial dependence between pixels is useful for classification.
- In all cases, the proposed method gives better results than the pixelwise methods.
- Novel spectral-spatial classification methods developed in this paper have a remarkable performance in terms of accuracy and reliability when compare with the previously recognized ECHO [2] and EMP [19].
- Uniformity based MRF showed a powerful tool to analyze the texture information is hyperspectral Images. Development approaches based on MRF to classify findings efficient and highly potent methods to classify different types of remote sensing images.
- The proposed method with weighting function leads to the rather prevent border provides better classification map. Therefore, these techniques are recommended for classification of hyperspectral images, especially for images containing large areas with unknown spectral features.
- In all cases, the weighting Markov Random Field margins in the proposed method gives better results than the proposed method.

REFERENCES

- [1] J. A. Richards, X. Jia, "Remote Sensing Digital Image Analysis: An Introduction," Springer-Verlag Berlin Heidelberg, 2006.
- [2] Kettig, R. L.; Landgrebe, D.A., "Classification of Multispectral Image Data by Extraction and Classification of Homogeneous Objects," *Geoscience Electronics, IEEE Transactions on*, vol.14, no.1, pp.19,26, Jan. 1976, doi: 10.1109/TGE.1976.294460
- [3] F. Bovolo and L. Bruzzone, "A context-sensitive technique based on support vector machines for image classification," First International Conference, PRMI 2005, Kolkata, India, December 20-22, 2005. DOI:10.1007/11590316_36
- [4] Desheng Liu, Maggi Kelly, Peng Gong, A spatial-temporal approach to monitoring forest disease spread using multi-temporal high spatial resolution imagery, *Remote Sensing of Environment*, Volume 101, Issue 2, 30 March 2006, Pages 167-180, ISSN 0034-4257, <http://dx.doi.org/10.1016/j.rse.2005.12.012>.
- [5] Ting-Fan Wu, Chih-Jen Lin, and Ruby C. Weng. 2004. Probability Estimates for Multi-class Classification by Pairwise Coupling. *J. Mach. Learn. Res.* 5 (December 2004), 975-1005.
- [6] C. Chang and C. Lin, "LIBSVM: A library for SVM" <http://www.csie.ntu.edu.tw/~cjlin/libsvm/> 2014.
- [7] Farag, A.A.; Mohamed, R.M.; El-Baz, A., "A unified framework for MAP estimation in remote sensing image segmentation," *Geoscience and Remote Sensing, IEEE Transactions on*, vol.43, no.7, pp.1617,1634, July 2005, doi: 10.1109/TGRS.2005.849059.
- [8] J. Platt, "Probabilistic outputs for Support Vector Machines and comparison to regularized likelihood methods," In A. Smola, P. Bartlett, B. Scholkopf, and D. Schuurmans, *Advances in Large Margin Classifiers* Cambridge, MA MIT Press., 2000.
- [9] Vladimir N. Vapnik. Statistical learning theory. Wiley, 1 edition, New York, September 1998.
- [10] Camps-Valls, G.; Bruzzone, L., "Kernel-based methods for hyperspectral image classification," *Geoscience and Remote Sensing, IEEE Transactions on*, vol.43, no.6, pp.1351,1362, June 2005, doi: 10.1109/TGRS.2005.846154
- [11] Licciardi, G.; Pacifici, F.; Tuia, D.; Prasad, S.; West, T.; Giacco, F.; Thiel, C.; Inglada, J.; Christophe, E.; Chanussot, J.; Gamba, P., "Decision Fusion for the Classification of Hyperspectral Data: Outcome of the 2008 GRS-S Data Fusion Contest," *Geoscience and Remote Sensing, IEEE Transactions on*, vol.47, no.11, pp.3857,3865, Nov. 2009, doi: 10.1109/TGRS.2009.2029340.
- [12] G. Noyel, J. Angulo, and D. Jeulin, "Morphological segmentation of hyperspectral images," *Image Analysis and Stereology*, pp. 26:101–109, 2007, doi: 10.5566/ias.v26.p101-109
- [13] Tarabalka, Y.; Chanussot, J.; Benediktsson, J.A.; Angulo, J.; Fauvel, M., "Segmentation and Classification of Hyperspectral Data using Watershed," *Geoscience and Remote Sensing Symposium, 2008. IGARSS 2008. IEEE International*, vol.3, no., pp.III - 652,III - 655, 7-11 July 2008, doi: 10.1109/IGARSS.2008.4779432
- [14] R.C. Gonzalez and R.E. Woods, "Digital Image Processing," Second Edition. Prentice Hall, 2002.
- [15] Geman, Stuart; Geman, D., "Stochastic Relaxation, Gibbs Distributions, and the Bayesian Restoration of Images," *Pattern Analysis and Machine Intelligence, IEEE Transactions on*, vol.PAMI-6, no.6, pp.721,741, Nov. 1984, doi: 10.1109/TPAMI.1984.4767596
- [16] A. H. Teller, and E. Teller, "Equations of state calculations by fast computing machines," *Journal of Chemical Physics*, pp. 21(6):1087–1092, 1953. doi: 10.1063/1.1699114
- [17] Tadjudin, S.; Landgrebe, D.A., "Covariance estimation with limited training samples," *Geoscience and Remote Sensing, IEEE Transactions on*, vol.37, no.4, pp.2113,2118, Jul 1999, doi: 10.1109/36.774728.
- [18] Benediktsson, J.A.; Kanellopoulos, I., "Classification of multisource and hyperspectral data based on decision fusion," *Geoscience and Remote Sensing, IEEE Transactions on*, vol.37, no.3, pp.1367,1377, May 1999, doi: 10.1109/36.763301
- [19] Antonio Plaza, Jon Atli Benediktsson, Joseph W. Boardman, Jason Brazile, Lorenzo Bruzzone, Gustavo Camps-Valls, Jocelyn Chanussot, Mathieu Fauvel, Paolo Gamba, Anthony Gualtieri, Mattia Marconcini, James C. Tilton, Giovanna Trianni, Recent advances in techniques for hyperspectral image processing, *Remote Sensing of Environment*, Volume 113, Supplement 1, September 2009, Pages S110-S122, ISSN 0034-4257, <http://dx.doi.org/10.1016/j.rse.2007.07.028>.
- [20] Tierney, Luke. "A note on Metropolis-Hastings kernels for general state spaces." *Annals of Applied Probability*, 1-9, 1998.
- [21] Pandolfi, Silvia, Francesco Bartolucci, and Nial Friel. "A generalization of the Multiplety Metropolis algorithm for Bayesian estimation and model selection." *International Conference on Artificial Intelligence and Statistics*. 2010. doi:10.1.1.207.2806
- [22] M. Borhani, H. Ghassemian, Novel Spatial Approaches for Classification of Hyperspectral Remotely Sensed Landscapes, *Symposium on Artificial Intelligence and Signal Processing*, December 2013.